

CONSTRAINTS ON THE SHAPE OF THE GALACTIC HALO FROM ACCURATE MEASUREMENTS OF PROPER MOTION OF HYPERVELOCITY STARS

OLEG Y. GNEDIN¹, WARREN R. BROWN²

(Dated: August 26, 2016)
To be submitted to ApJ

ABSTRACT

We present predictions for a future astrometric mission...

Keywords: stars: early-type — Galaxy: halo — Galaxy: kinematics and dynamics

1. INTRODUCTION

Hypervelocity stars (HVSs) are unbound stars ejected from the Galaxy by the Milky Way’s central massive black hole (MBH) (Hills 1988; Brown 2015). First discovered by Brown et al. (2005), there are now 21 unbound main sequence B-type stars whose properties are best explained by this origin (Brown et al. 2014). HVSs importantly connect the center of the Milky Way to the outer halo. Launched on radial trajectories from the Galactic center, HVSs integrate the gravitational potential of the Milky Way as they travel to 100 kpc distances. DM discussion.

...If the mass distribution of the Milky Way is non-spherical, the trajectories of the HVSs must deviate from being precisely radial...

There are now many lines of evidence to support the Galactic center origin of HVSs. Following the first discovery, Brown et al. (2007, 2014) performed a complete spectroscopic survey of halo stars with the colors of $3 M_{\odot}$ stars. The color-selected survey found 21 stars unbound in radial velocity alone, plus a comparable number of outliers with bound velocities. The bound and unbound velocity outliers all move outwards, consistent with an ejection origin, and the distribution of velocities is consistent with expectations from the Hills mechanism (Kenyon et al. 2008, 2014). The number of unbound B-type stars is also consistent with theoretically predicted ejection rates (Hills 1988; Zhang et al. 2010, 2013). Follow-up echelle observations establish that the unbound stars are rapid rotators $55 < v \sin i < 320 \text{ km s}^{-1}$ and thus main-sequence B stars (Przybilla et al. 2008; López-Morales & Bonanos 2008; Brown et al. 2012a, 2013). The difference between their estimated ages and flight times is 100 Myr, a timescale inconsistent with scenarios that require prompt ejection, such as supernovae, but consistent with a Galactic center origin (Brown et al. 2012a). While extreme supernova ejections can overlap in velocity with HVSs (Heber et al. 2008), high velocity ejections from the disk will have a strong Galactic latitude dependence because of the rotation of the disk (Bromley et al. 2009). Observed unbound B stars are spread uniformly over Galactic latitude, inconsistent with a disk origin but consistent with a Galactic center origin (Brown et al. 2012b). The Milky Way’s MBH must eject HVSs, and only the MBH ejection can self-consistently explain the the number, velocity, stellar nature, flight time, and spatial distribution of the observed unbound B stars.

Further evidence for the Galactic center origin of HVSs is found in the Galactic center. Several dozen B-type stars orbit within about 0.04 pc of the MBH on randomly oriented, eccentric orbits (the so-called S stars) (Ghez et al. 2008; Gillessen et al. 2009). Spectroscopy establishes that the S stars are normal main-sequence B stars (Ghez et al. 2003; Eisenhauer et al. 2005). The tidal forces of the MBH are too strong to permit star formation in these close orbits (Morris 1993), thus the short-lived B must form elsewhere and then be captured next to the MBH (Gould 2003).

The same three-body exchange that ejects a HVS also captures a star onto a tight, eccentric orbit around the MBH, thus the S stars are the likely former companions of HVSs. The number of S stars is consistent with the number of unbound B stars in the halo (Bromley et al. 2012; Kenyon et al. 2014). The distribution of S star eccentricities matches predictions of the Hills mechanism (Perets 2009; Zhang et al. 2013; Madigan et al. 2014). Stars at larger radii from the MBH have increasingly eccentric orbits, consistent with their being captured by the Hills mechanism onto orbits with longer relaxation times (Madigan et al. 2014). Thus the number, orbital distribution, and stellar nature of stars orbiting the central MBH supports the HVS ejection mechanism.

2. WHAT AFFECTS THE EXPECTED TANGENTIAL MOTION

2.1. Flattening of stellar distribution

2.2. Halo triaxiality

Fig 1: Cartoon of proper motions for two different orientations of dark matter halo (prolate vs. oblate) that match the observed vlos and position, to illustrate figure 2

2.3. New fit to mass model

Fig 2: mass distribution in the adopted Galactic model with existing observations

3. EXPECTED PROPER MOTION

calculate expected proper motion for different orientation of the triaxial halo

¹ Department of Astronomy, University of Michigan, Ann Arbor, MI 48109, USA

² Smithsonian Astrophysical Observatory, 60 Garden St, Cambridge, MA 02138, USA

Table 1
UNBOUND HYPERVELOCITY STARS

ID	RA, Dec (J2000)	g_0 (mag)	d_{helio} (kpc)	v_{helio} (km s ⁻¹)	$\mu_{\text{RA}}, \mu_{\text{Dec}}$ (mas yr ⁻¹)
HVS 1	9:07:44.99, +02:45:06.9	19.69 ± 0.023	102 ± 15	831.1 ± 5.7	$+0.08 \pm 0.26, -0.12 \pm 0.22$
HVS 4	9:13:01.00, +30:51:19.9	18.34 ± 0.023	64 ± 9.8	600.9 ± 6.2	$-0.23 \pm 0.36, -0.42 \pm 0.36$
HVS 5	9:17:59.47, +67:22:38.3	17.58 ± 0.032	45 ± 5.2	545.5 ± 4.3	$+0.55 \pm 0.61, -0.44 \pm 0.59$
HVS 6	11:05:57.45, +09:34:39.4	18.94 ± 0.024	55 ± 6.9	609.4 ± 6.8	$+0.05 \pm 0.57, +0.31 \pm 0.97$
HVS 7	11:33:12.13, +01:08:24.8	17.63 ± 0.015	52 ± 6.4	526.9 ± 3.0	$+1.00 \pm 0.82, -0.55 \pm 1.04$
HVS 8	9:42:14.03, +20:03:22.0	17.93 ± 0.016	53 ± 9.8	499.3 ± 2.9	$-0.82 \pm 1.16, -0.04 \pm 0.49$
HVS 9	10:21:37.08, -00:52:34.7	18.64 ± 0.023	74 ± 12	616.8 ± 5.1	$-1.26 \pm 0.74, -0.25 \pm 0.70$
HVS 10	12:03:37.85, +18:02:50.3	19.24 ± 0.024	52 ± 5.8	467.9 ± 5.6	$-1.07 \pm 0.36, -0.58 \pm 0.42$
HVS 12	10:50:09.60, +03:15:50.6	19.63 ± 0.024	66 ± 8.5	552.2 ± 6.6	$-0.40 \pm 0.36, +0.31 \pm 0.34$
HVS 13	10:52:48.31, -00:01:33.9	20.01 ± 0.021	105 ± 19	569.3 ± 6.1	$-0.90 \pm 0.38, +0.46 \pm 0.44$
HVS 14	10:44:01.75, +06:11:39.0	19.72 ± 0.023	102 ± 16	537.3 ± 7.2	...
HVS 15	11:33:41.09, -01:21:14.2	19.15 ± 0.020	66 ± 9.6	461.0 ± 6.3	...
HVS 16	12:25:23.40, +05:22:33.8	19.33 ± 0.029	71 ± 12	429.8 ± 7.0	...
HVS 17	16:41:56.39, +47:23:46.1	17.43 ± 0.015	50 ± 4.4	250.2 ± 2.9	...
HVS 18	23:29:04.95, +33:00:11.4	19.30 ± 0.015	77 ± 11	237.3 ± 6.4	...
HVS 19	11:35:17.76, +08:02:01.4	20.06 ± 0.035	97 ± 15	592.8 ± 11.8	...
HVS 20	11:36:37.13, +03:31:06.8	19.81 ± 0.025	75 ± 11	512.1 ± 8.5	...
HVS 21	10:34:18.25, +48:11:34.5	19.73 ± 0.030	108 ± 21	356.8 ± 7.5	...
HVS 22	11:41:46.45, +04:42:17.2	20.18 ± 0.042	84 ± 13	597.8 ± 13.4	...
HVS 23	21:56:29.02, +00:54:44.1	20.20 ± 0.027	115 ± 20	259.3 ± 9.8	...
HVS 24	11:11:36.44, +00:58:56.4	18.86 ± 0.016	54 ± 7.5	492.5 ± 5.3	...

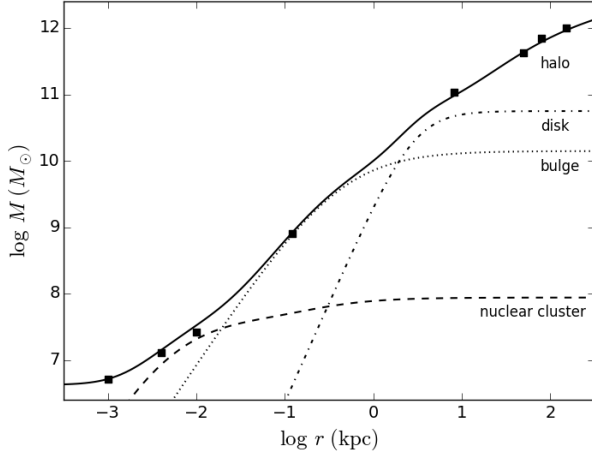


Figure 1. New model of mass distribution in the Galaxy.

Fig 3: Spread of proper motion for one star

Fig 4: Constraints on axis ratios without and with distance information (20% distance error) for one star (HVS 5)

Fig 5: Same for overlapping contours of two stars (HVS 5 and 4 or 9)

and/or Fig 6: Same for central bands (tiny p.m. error) for all stars, to illustrate which stars are best and what can be gained from a larger sample

OLEG TO DO: quantitative way to combine several measurements expected from Gaia; write down full likelihood; check if joint constraints could be tighter than naive overlap of contours

4. DISCUSSION

Gaia Data Release 2 at the end of 2017 will have too large uncertainty

argue for future space-based astrometric mission with large FOV to include enough quasars and reach high enough accuracy of p.m.

complementary probes of halo shape; current constraints

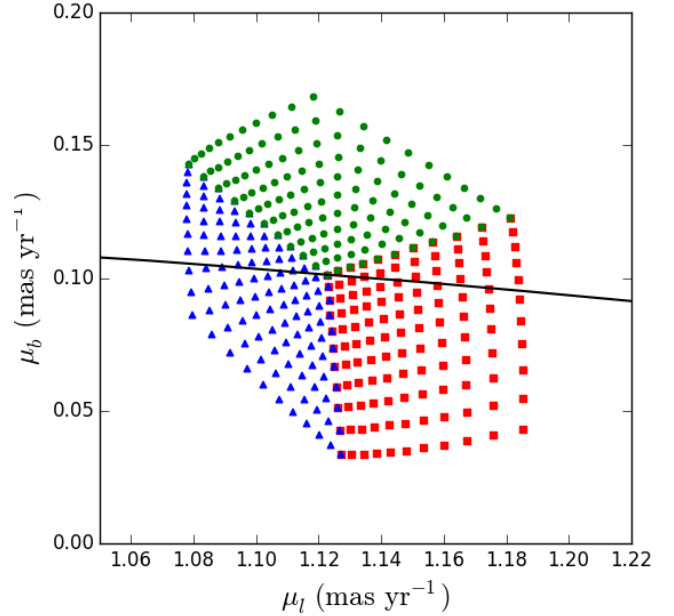


Figure 2. Spread of expected proper motions for different configurations of the triaxial dark matter halo.

are consistent with spherical
and at larger distances than tidal streams

5. CONCLUSION

test of dark matter physics
robust test of CDM model predictions
requires future, more accurate mission to do it

6. SUMMARY

We

This research makes use of SAO/NASA's Astrophysics

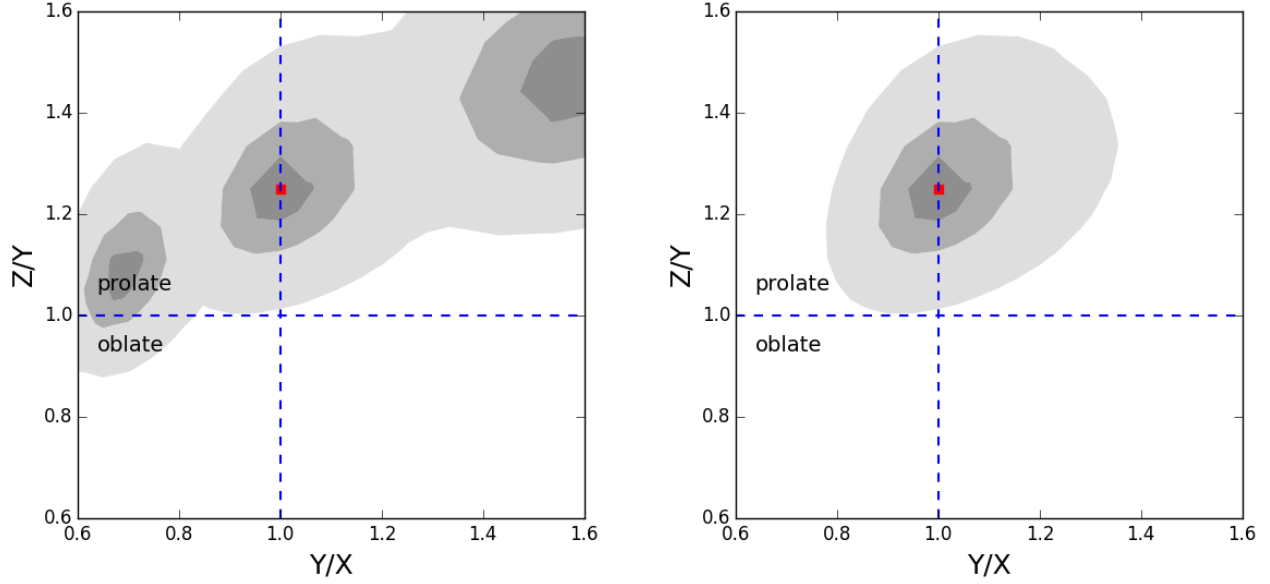


Figure 3. Constraints on axis ratios of the triaxial dark matter halo for one star with (*right panel*) and without (*left panel*) distance information.

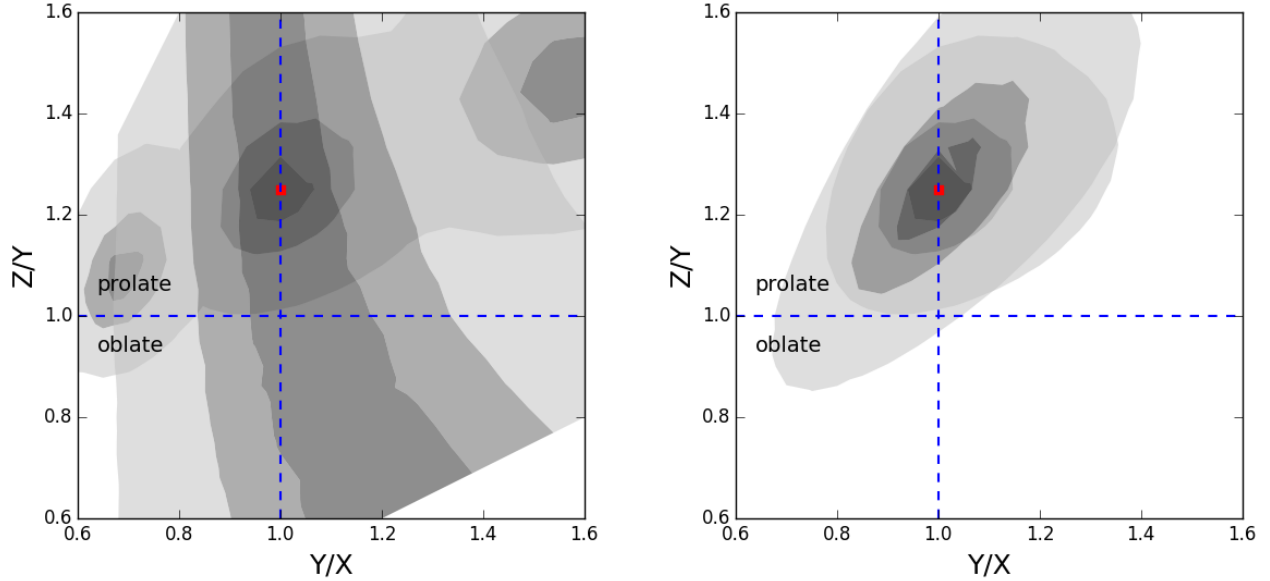


Figure 4. Constraints on axis ratios of the triaxial dark matter halo for two stars with (*right panel*) and without (*left panel*) distance information.

Data System Bibliographic Services. This work was supported in part by the Smithsonian Institution. O.G. was

supported in part by NASA through grant NNX12AG44G, and by NSF through grant AST-1412144.

REFERENCES

- Bromley, B. C., Brown, W. R., Geller, M. J., & Kenyon, S. J. 2009, *ApJ*, 706, 925
 Bromley, B. C., Kenyon, S. J., Geller, M. J., & Brown, W. R. 2012, *ApJL*, 749, L42
 Brown, W. R. 2015, *ARA&A*, 53, 15
 Brown, W. R., Cohen, J. G., Geller, M. J., & Kenyon, S. J. 2012a, *ApJL*, 754, L2
 —. 2013, *ApJ*, 775, 32
 Brown, W. R., Geller, M. J., & Kenyon, S. J. 2012b, *ApJ*, 751, 55
 —. 2014, *ApJ*, 787, 89
 Brown, W. R., Geller, M. J., Kenyon, S. J., & Kurtz, M. J. 2005, *ApJL*, 622, L33
 Brown, W. R., Geller, M. J., Kenyon, S. J., Kurtz, M. J., & Bromley, B. C. 2007, *ApJ*, 671, 1708
 Eisenhauer, F., Genzel, R., Alexander, T., et al. 2005, *ApJ*, 628, 246
 Ghez, A. M., Salim, S., Weinberg, N. N., et al. 2008, *ApJ*, 689, 1044
 Ghez, A. M. et al. 2003, *ApJL*, 586, L127
 Gillessen, S., Eisenhauer, F., Trippe, S., et al. 2009, *ApJ*, 692, 1075

- Gould, A. 2003, *ApJL*, 592, L63
- Heber, U., Edelmann, H., Napiwotzki, R., Altmann, M., & Scholz, R.-D. 2008, *A&A*, 483, L21
- Hills, J. G. 1988, *Nature*, 331, 687
- Kenyon, S. J., Bromley, B. C., Brown, W. R., & Geller, M. J. 2014, *ApJ*, 793, 122
- Kenyon, S. J., Bromley, B. C., Geller, M. J., & Brown, W. R. 2008, *ApJ*, 680, 312
- López-Morales, M. & Bonanos, A. Z. 2008, *ApJL*, 685, L47
- Madigan, A.-M., Pfuhl, O., Levin, Y., et al. 2014, *ApJ*, 784, 23
- Morris, M. 1993, *ApJ*, 408, 496
- Perets, H. B. 2009, *ApJ*, 690, 795
- Przybilla, N., Nieva, M. F., Tillich, A., et al. 2008, *A&A*, 488, L51
- Zhang, F., Lu, Y., & Yu, Q. 2010, *ApJ*, 722, 1744
- . 2013, *ApJ*, 768, 153